

## NANOSTRUCTURE PROPERTIES AND DYE-SENSITIZED-SOLAR-CELL OPEN-CIRCUIT VOLTAGE OF A TiO<sub>2</sub> AEROGEL AND PRE-HYDROTHERMALLY TREATED XEROGELS

Bambang Priyono<sup>1\*</sup>, Akhmad Herman Yuwono<sup>1</sup>, Badrul Munir<sup>1</sup>, Muhammad Hasan Mustofa<sup>1</sup>, Faizah<sup>1</sup>

<sup>1</sup>*Department of Metallurgical and Materials Engineering, Faculty of Engineering, Universitas Indonesia, Kampus UI Depok, Depok 16424, Indonesia*

(Received: December 2017 / Revised: March 2018 / Accepted: July 2018)

### ABSTRACT

Dye-sensitized solar cells (DSSCs) are third-generation photovoltaic devices, which are considered to be a very promising renewable-energy source that offers an alternative to fossil fuels due to their low cost, ease of production, and eco-friendliness. One of the most important components in DSSCs is the TiO<sub>2</sub> layer, which serves as an active inorganic semiconductor oxide for photoelectron activity. Herein, TiO<sub>2</sub> nanoparticles were synthesized via a sol-gel process using titanium tetra-n-butoxide, ethanol, hydrochloric acid, and deionized water at molar ratios of 0.4:0.83:1:1.39 upon sol preparation, followed by hydrothermal processes at three different temperatures (i.e., 100°C, 120°C, and 150°C); ambient drying; and multi-step calcination. For comparison, TiO<sub>2</sub> aerogel nanoparticles were also prepared via supercritical extraction followed by multi-step calcination. The samples were analyzed by X-ray diffraction, Brunauer–Emmett–Teller surface-area measurements, UV–Vis spectroscopy in the diffuse-reflectance mode, and scanning electron microscopy. The results showed that the pre-hydrothermally treated samples exhibited band-gap energies of 3.34, 3.29, and 3.32 eV after treatment at 100°C, 120°C, 150°C, respectively, whereas the aerogel sample had a band-gap energy of 3.33 eV. Open-circuit-voltage measurements revealed that the DSSCs fabricated by pre-hydrothermal treatment at 120°C generated a higher voltage (320 mV) than aerogel cells (21 mV).

**Keywords:** Aerogel; Multi-step calcination; Open circuit voltage; Pre-hydrothermal treatment; Supercritical extraction

### 1. INTRODUCTION

The use of renewable energy is a key way to overcome the world's energy crisis. Dye-sensitized solar cells (DSSCs) are one of the most attractive solar-energy harvesting methods due to their low cost, high photon conversion efficiency, and good stability (O'Regan & Grätzel, 1991). Many efforts have been made to improve the performance of DSSCs (Khan et al., 2017) with an important approach being the optimization of the photoanode. In this case, the performance improvement relates to the base material, which is influenced by the structure of the oxide layer having a high surface area to absorb sensitizing dyes and maximize the performance as required. One of the most commonly used semiconductor layers in DSSCs is TiO<sub>2</sub> (Sofyan et al., 2017). TiO<sub>2</sub> nanoparticles have gained importance for the fabrication of photoanodes, which

---

\*Corresponding author's email: bambang.priyono@ui.ac.id, Tel. +62-21-7863510, Fax. +62-21-7872350  
Permalink/DOI: <https://doi.org/10.14716/ijtech.v9i5.1067>

comprise a monolayer of highly porous material (Sugathan et al., 2015). The photoelectrode in a DSSC is sometimes also referred to as the working electrode, and under commercial development, it generally includes titania nanoparticles. The crystal phase of the TiO<sub>2</sub> particles used in DSSCs is generally the anatase phase because of its high dye-absorbance properties (Nursama & Muliani, 2012).

In addition, the use of TiO<sub>2</sub> is excellent from the viewpoint of its optical properties because it has a band-gap energy of ~3.2 eV with a wavelength of <380 nm (Langlet et al., 2002). Furthermore, the crystallinity and high-surface-area properties of the TiO<sub>2</sub> anatase nanostructure are preferred due to the high photoactivity of the material. Many studies are focusing on the methods to prepare TiO<sub>2</sub> to meet the required properties for photoanodes, e.g., by solid-state, sol-gel routes with various thermal treatments. The sol-gel method is one of the most useful techniques for synthesizing nanoparticles with high purity of precursor to obtain a high surface area, large pore volume, and uniform pore-size distribution.

A hydrothermal treatment was applied here to prepare TiO<sub>2</sub> anatase [instead of the supercritical extraction (SCE) method] because it offers several advantages, including high purities, a good distribution of the material, and increased photoactivity and crystallite size (Dai et al., 2010). Earlier studies on hydrothermal synthesis have shown good results for titanium-tetra-isopropoxide, which exhibited an open circuit voltage of 69.33 mV and a crystallite size of 12.46 nm (Yuwono et al., 2010). In contrast, the SCE technique involves CO<sub>2</sub> as the extraction solvent, which has the potential to augment the surface area of the nanoparticles but may also lead to a low degree of crystallinity. Thus, to overcome the crystallinity issue, both of them must be calcinated at various temperatures and different conditions. A modification of the simple nanostructure-synthesis process used in this study to obtain TiO<sub>2</sub> is the bottom-up method (sol-gel), as described above, which includes supercritical and hydrothermal treatments followed by gradual calcination. Synthesizing nanoparticles using the sol-gel method can improve the properties of TiO<sub>2</sub> structures regarding the degree of crystallinity, surface area, and photoactivity. Therefore, this study aims at designing a better preparation technique for optimum results, perform both treatments to improve the crystallite structure, and reduce the size of the band-gap-energy (Kim et al., 2007), coupled with a gradual calcination in some condition.

In our previous study, TiO<sub>2</sub> nanoparticles were successfully synthesized from titanium tetra-n-butoxide using the sol-gel method, followed by supercritical extraction and multi-step calcination, to obtain a highly crystalline aerogel with a vast surface area and increased photoelectrochemical sensitivity (Priyono et al., 2013). In the present study, the preparation technique has been modified to improve the nanostructure properties for use in DSSC devices. The method uses a xerogel combined with a hydrothermal process and followed by multi-step calcination to improve the crystallinity of all the samples while maintaining a minimum loss in surface area due to crystal growth. The results were then compared to those obtained for a TiO<sub>2</sub> aerogel prepared by the SCE method with the same multi-step calcination process as that demonstrated by (Brodsky & Ko, 1994).

The correlation between TiO<sub>2</sub> nanostructure properties such as crystallite size, surface area, and band-gap energy and the performance of the material as a semiconductor for better and more efficient DSSCs was investigated.

## 2. METHODS

First, a TiO<sub>2</sub> sol was prepared by hydrolysis of titanium tetra-n-butoxide (Kanto Chemical, Japan) by dropwise addition of a mixture of hydrochloric acid and water in an ethanol solution under vigorous stirring to obtain a transparent sol solution. The molar ratio of titanium tetra-n-

butoxide, ethanol, hydrochloric acid, and deionized water was 0.4:0.83:1:1.39. The mixture was stirred for three hours to stabilize the solution and then sealed in a container for 1–2 days at room temperature.

The gels were processed in two different ways: In the first route, they were treated hydrothermally in a Teflon-lined stainless-steel autoclave (Parr-Moline, Illinois USA) equipped with a specially modified sample holder, sealed, and placed in an oven at different temperatures of 100°C, 120°C, and 150°C for 14 hours. Then, they were dried at 70°C for 24 hours in a drying oven and subjected to a three-stage (multi-step) calcination process at 150°C, 300°C, and 420°C for one hour each in a tube furnace to improve the crystallinity. The first and second stages of the multi-step calcination process took place under vacuum conditions, whereas the last stage included injecting air to the system to obtain a white powder composed of TiO<sub>2</sub> nanoparticles. The first stage of the multi-step calcination process occurs at 150°C, a temperature at which the solvent evaporates. The second stage takes place at 300°C to remove any remaining organic compounds, and the final stage occurs at 420°C under air input to oxidize the sample and obtain white TiO<sub>2</sub> powder. In the second route, the gels were further processed into aerogels by SCE in an extractor at an extraction pressure of 1500 psi and a temperature of 50°C for two hours. During this SCE procedure, the solvent in the mixed sol-gel was separated using CO<sub>2</sub> gas at its critical point of 31.1°C. In this process, the sol-gel was inserted directly into the washed steel pressure vessel and then into the autoclave. The resulting product was calcinated in three stages to improve its crystallinity. The two TiO<sub>2</sub> gels obtained from these processes had a white/opaque and glass-like appearance, respectively.

The samples treated by the pre-hydrothermal and SCE processes were characterized by X-ray diffraction (XRD, Bruker AXS  $\theta$ – $2\theta$ ) to identify the TiO<sub>2</sub> anatase phase and determine the crystallite size through Scherrer's equation. For phase-identification purposes, an XRD-pattern analysis was performed using the X'Pert High Score Plus software based on the JCPDS 21-1272 reference numbers. Brunauer–Emmet–Teller (BET) (Quantachrome NOVA 1200e) tests were performed to determine the surface area; UV–Vis diffuse-reflectance spectroscopy (DRS, Shimadzu UV-2401PC) measurements were performed to determine the band-gap energy, which was calculated through the Kubelka–Munk function using a Tauc equation analysis; and scanning electron microscopy (SEM) images were taken to determine the morphology of the TiO<sub>2</sub> structures. The performance of DSSCs assembled from nanoparticles resulting from both methods was tested by measuring the open circuit voltage ( $V_{oc}$ ) under the light beam of an overhead projector.

### 3. RESULTS AND DISCUSSION

The XRD patterns of hydrothermal samples obtained at 100, 120, and 150°C are shown in Figure 1, whereas the pattern of an aerogel sample is presented in Figure 2.

As shown in Figure 1, the three pre-hydrothermally treated samples exhibit distinct peaks, indicating that the amorphous phase was successfully transformed into the crystalline anatase phase after calcination at 420°C. Based on these results, it can be confirmed that multi-step calcination successfully enhances the nano-crystallinity of the TiO<sub>2</sub> phase. Figures 1 (A), (B), and (C) show the XRD patterns of as-prepared TiO<sub>2</sub> powders treated at different temperatures (i.e., 100°C, 120°C, and 150°C). Peaks are observed at  $2\theta$  values of 25.65°, 37.60°, 38.95°, 48.37°, 54.23°, 55.60°, 63.20°, 68.99°, 70.78°, and 75.37°, and can be assigned, respectively, to the (101), (004), (112), (200), (105), (211), (204), (116), (220), and (215) lattice planes of the TiO<sub>2</sub> anatase phase (JCPDS Card no. 21-1272). The well-formed peaks clearly show that the anatase phase was successfully formed by multi-step calcinations at 150°C, 300°C, and 420°C. Surface-area measurements based on the BET method show a further advantage of the multi-

step calcination process, which minimizes the decrease in surface area of the anatase  $\text{TiO}_2$  material as a consequence of crystallite growth and pore enlargement.

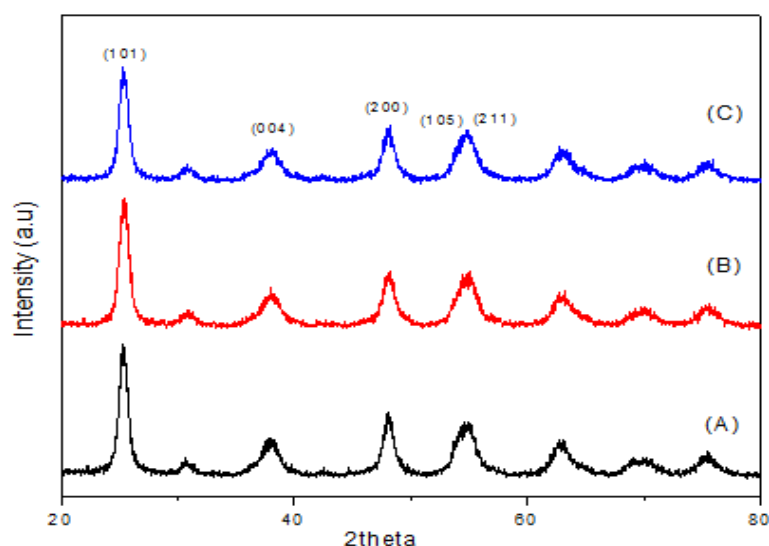


Figure 1 XRD patterns of calcined hydrothermal samples obtained at: (A) 100°C; (B) 120°C; and (C) 150°C

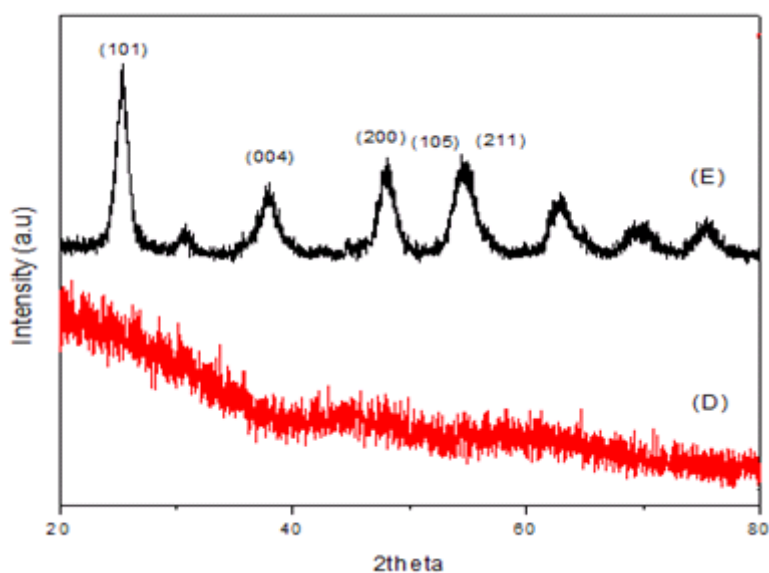


Figure 2 XRD patterns of: (D) an as-dried aerogel; and (E) a calcined aerogel

The very shallow hump in Figure 2 shows that the as-dried aerogel (sample D) has an amorphous phase. However, after calcination at 420°C, the anatase phase was formed (sample E), as confirmed by the presence of higher diffraction peaks indicating an enhanced nanocrystallinity. For the hydrothermally treated samples, increasing the hydrothermal temperature from 100°C to 150°C also resulted in higher diffraction peaks. This is triggered by the temperature of the process that allows the Ti–O–Ti nuclear cluster to grow uniformly assisted by the evaporation process of water so that the dispersion of the increasing size of the crystallite diameter is more widespread (Wang & Ying, 1999), although the hydrothermal process takes a long time. In contrast to the SCE process, the crystallite size barely increases upon multi-step calcination. Thus, the XRD patterns of the resulting SCE samples indicate a slightly high crystallinity but not higher than that of the materials obtained by the hydrothermal process, as

explained above. However, one of the benefits of the SCE process is that it can be finished within two hours. In addition, the resulting surface area is higher than that of the structures obtained by the hydrothermal process followed by calcination (Schneider & Baiker, 1997).

As shown in Figure 3, the broadening of the peaks in the XRD pattern was analyzed to estimate the crystallite size. This was done by determining the widening at half the intensity of the diffraction peak (or full width at half maximum, FWHM) using the Scherrer equation, as summarized in the comparison diagram. Well-defined peaks indicate the formation of the anatase phase by multi-step calcination at temperatures of 150°C, 300°C, and 420°C. FWHM in each pre-hydrothermal and aerogel samples processed using SCE process to estimate the average size of crystallite size diameter after calcination, whether the TiO<sub>2</sub> anatase of this works still has the nano-size crystallite.

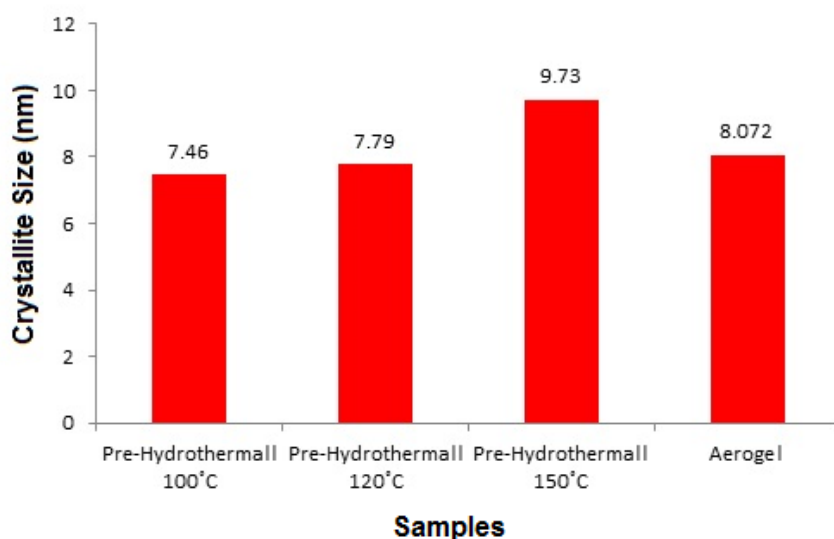


Figure 3 Comparison of the crystallite size of samples obtained under different conditions

In Figure 3, the crystallite size is sorted from small to large according to the rise in the process temperature for the pre-hydrothermal samples, that is, 7.46, 7.79, and 9.73 nm. It can be seen that the higher the process temperature, the larger the crystallite size (Naghibi et al., 2014). For comparison, the crystallite size of the TiO<sub>2</sub> aerogel sample was 8.07 nm.

As can be seen in Figure 3, the hydrothermal process at 150°C and the SCE procedure result in the largest average crystallite sizes. This is because pre-hydrothermal treatment at 150°C plays a specific role in suppressing the development of rigid Ti–OH networks, which represent an obstacle for TiO<sub>2</sub>-crystallite growth. Increasing the timeframe of the pre-hydrothermal process can reduce the number of rigid Ti–OH networks responsible for the formation of highly amorphous and low crystalline TiO<sub>2</sub> phases (Yuwono et al., 2006). The suppression of rigid networks results in a complete hydrolysis, which makes the Ti–OH networks more flexible, thus facilitating the preparation and densification of Ti–O–Ti bonds and enhancing the crystallinity of TiO<sub>2</sub>, which is better than that of materials obtained by the SCE process. This leads to an increase in the crystallite size of the hydrothermally treated samples. For the hydrothermal process at 120°C, the crystallite size was close to that of the structures obtained by SCE. This indicates that the diffusion process during re-arrangement of the TiO<sub>2</sub> nanocrystalline structures is not fast enough and has not been completed within the predetermined time. Lastly, for the hydrothermal process at 100°C, the crystallite size was below that of the SCE materials, confirming the previous results.

The results of BET surface-area measurements for various samples after multi-step calcination are summarized in Table 1. The surface-area properties of photoanodes play an important role in determining the dye-absorbing properties of these materials during DSSC assembly.

The BET measurements indicate how effective the multi-step calcination process is in minimizing the decrease in surface area of the nanoparticles while improving their crystallinity. Multi-step calcination results in a higher surface area compared to conventional calcination because it prevents the collapse of pore networks due to the high process temperature (Priyono et al., 2013).

Table 1 Surface area of samples after multi-step calcination

Sample Code	Degassing Condition	BET Surface Area (m <sup>2</sup> /g)
Aerogel	100°C–3 hours	110.31
Pre-Hydrothermal 100°C	100°C–3 hours	71.30
Pre- Hydrothermal 120°C	100°C–3 hours	85.43
Pre- Hydrothermal 150°C	100°C–3 hours	82.17

Table 1 shows that the aerogel process leads to nanoparticle samples with a much higher surface area compared to the other three processes. The CO<sub>2</sub> gas suppressed in the critical temperature and critical pressure is able to remove the solvent from the sol-gel within the autoclave, thus leaving dry porous gel networks and increasing the surface area of the pores. After multi-step calcination, which is necessary for improving the crystallinity of the samples, the surface area increases, contributing to the absorption process for DSSC applications. Thus, it is important to minimize the decrease in surface area during thermal treatment—caused by pore enlargement—which is why calcination is performed in a multi-step fashion, rather than in a single continuous way.

Figure 4 shows the UV–Vis reflectance spectra of the prepared samples. This UV–Vis DRS characterization was performed to study the optical response of the synthesized nanocrystalline TiO<sub>2</sub> particles.

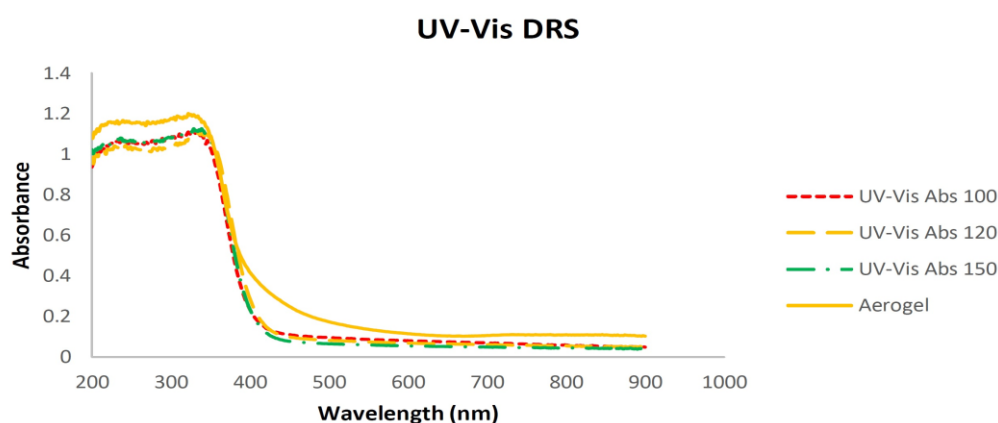


Figure 4 Comparison of the reflectance spectra of a TiO<sub>2</sub> aerogel and pre-hydrothermally treated xerogels

Figure 4 indicates a slight red shift of the signals for the pre-hydrothermally treated samples upon increasing the temperature from 100°C to 120°C. However, the spectrum of the sample prepared at 150°C shows a blue shift. The aerogel follows the same trend as the pre-hydrothermal sample obtained at 150°C. It would be interesting to correlate the shifting tendency to the crystallite diameter, but this requires further work.

Figure 5 shows the band-gap energies determined for the different samples using the Kubelka–Munk equation.

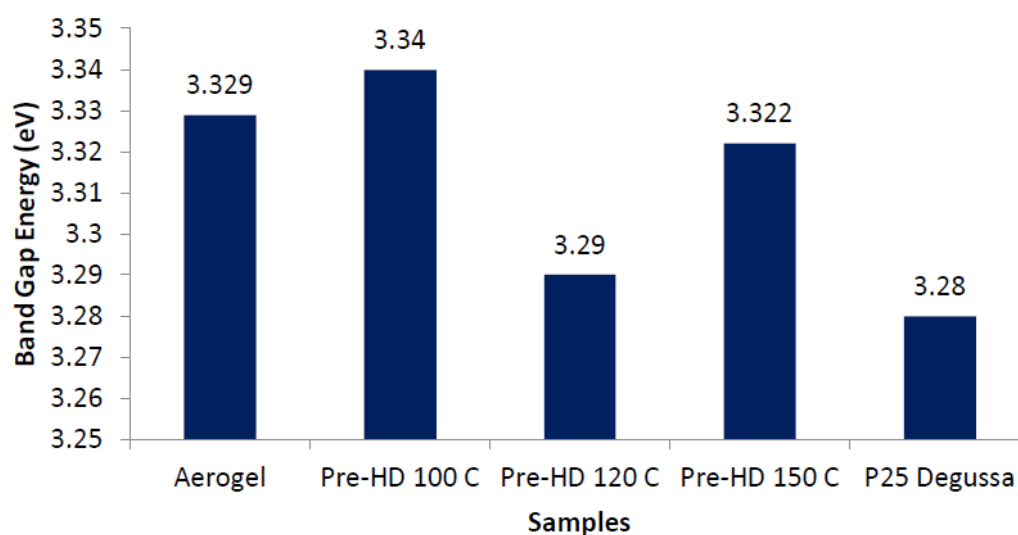


Figure 5 Comparison of the band-gap energies of pre-hydrothermally treated and aerogel samples

The sample that was pre-hydrothermally treated at 120°C has the lowest band-gap energy, namely, 3.29 eV, which is close to the band-gap-energy yield for the synthesis of anatase phase TiO<sub>2</sub> (3.28 eV) (Slamet et al., 2005). A lower band gap indicates a higher crystallinity of the samples. It is also related to the crystallite size with bigger crystallites leading to a lower band-gap energy. In Figure 5, however, it is shown that the higher crystallite size of the pre-hydrothermal sample prepared at 150°C does not lead to the lowest band-gap energy. This result needs to be investigated further and may indicate that the optimum parameters are already reached for the pre-hydrothermal treatment at 120°C. The band gap may also be affected by the particle diameter, which is determined by agglomeration and densification mechanisms occurring when the sample is subjected to higher process temperatures. The shape and size of the particles can be investigated by SEM.

Structure and morphology analyses of the samples were performed by SEM, as shown in Figure 6. The magnifications used for each sample varied from 1,000× (to see particles and the presence of agglomerates) to 50,000× (to show the diameters of tiny particles besides the agglomerates).

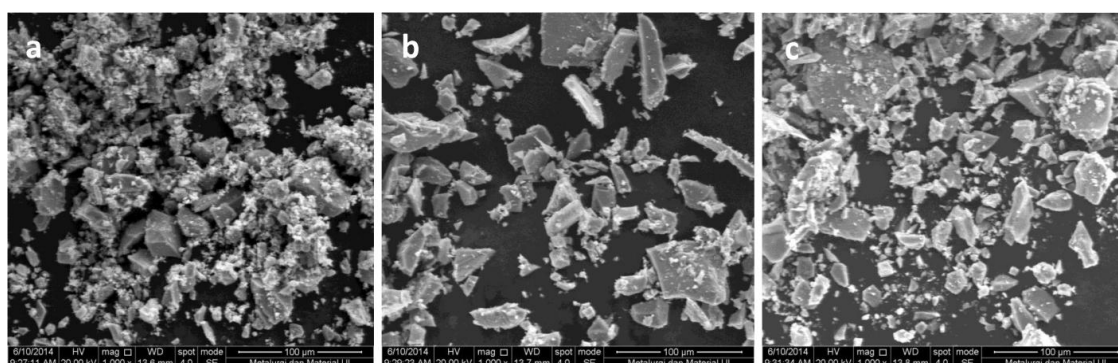


Figure 6 SEM images of hydrothermal samples prepared at: (a) 100°C; (b) 120°C; and (c) 150°C (scale-bar: 100 µm)

Figure 6 shows the sizes and morphologies of the studied  $\text{TiO}_2$  particles. Higher hydrothermal-treatment temperatures lead to coarser agglomerates. To maximize the application of SEM in characterizing the influence of the temperature during hydrothermal treatment, images at 50000 $\times$  magnification were also taken, as shown in Figures 7, 8, and 9.

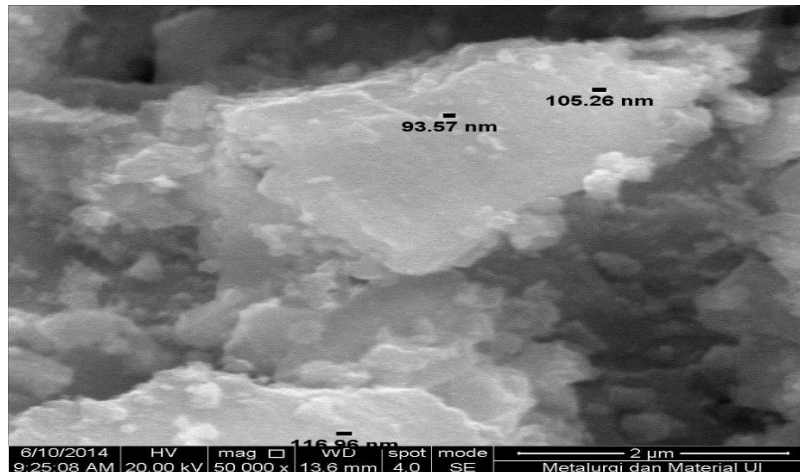


Figure 7 SEM image showing the tiny particle sizes in a pre-hydrothermally treated sample prepared at 100°C

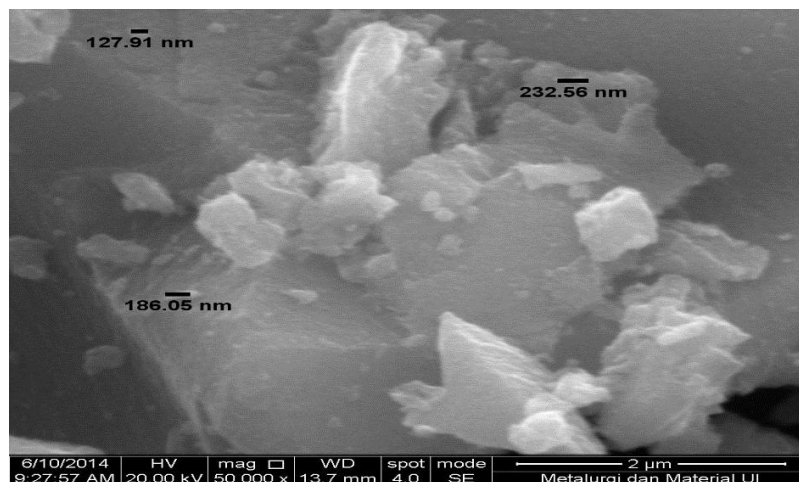


Figure 8 SEM image showing the tiny particle sizes in a pre-hydrothermally treated sample prepared at 120°C

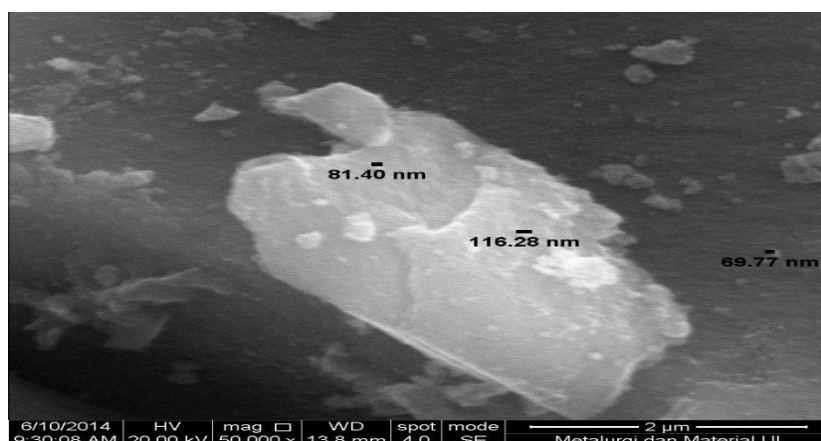


Figure 9 SEM image showing the tiny particle sizes in a pre-hydrothermally treated sample prepared at 150°C

Figures 7, 8, and 9 show SEM images including scale-marks on tiny particles located beside large agglomerates. The morphologies and roughness of TiO<sub>2</sub> particles obtained at various treatment temperatures can also be observed. At 100°C treatment, the obtained particles consist of sharp and rough structures with sizes between 94 and 105 nm. At 120°C treatment, the shapes and edges of the particles become smoother and their size increases to 127, 186, and 233 nm. Finally, at 150°C, the shapes and edges are completely smooth (with no remaining sharp corners), but the sizes of the particles decrease again to 81 and 116 nm, despite the coarsening phenomenon.

Although understanding the influence of the temperature during the hydrothermal treatment is complicated, using the sizes of tiny particles beside agglomerates may provide a good approximation of the shape and size of the TiO<sub>2</sub> particles resulting from the treatment. The shape of surface particles also changes with increasing temperature; their structure becomes smoother as a result of densification. These findings are largely in line with the observed increase in particle size upon increasing the temperature of the hydrothermal synthesis process (Ge et al., 2006). Generally, a high average crystallite size increases the particle size, but not always, and therefore, the correlation between surface-area decrease and band-gap energy is strongly influenced by the particle size (Kim et al., 2007).

In this work, the DSSC performance of the samples was examined by open voltage circuit (Voc) measurements upon exposure to a 50-W projector lamp. The results of the measurement are shown in Figure 10.

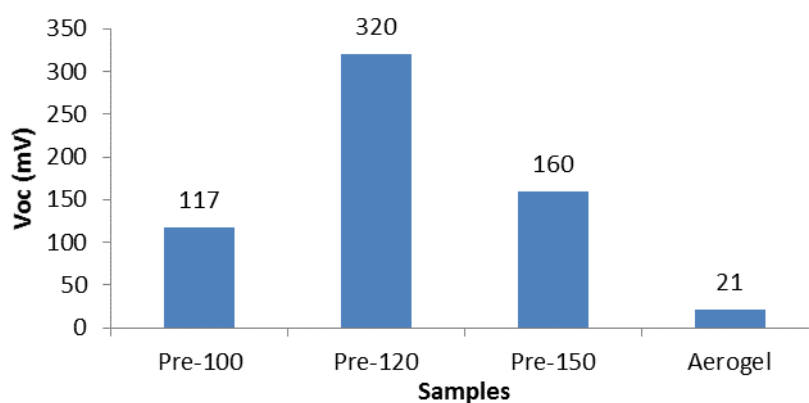


Figure 10 Open-circuit-voltage comparison between pre-hydrothermally treated and aerogel samples

As shown in Figure 10, the pre-hydrothermal sample treated at 120°C has the highest Voc value (320 mV) and a band-gap energy of 3.290 eV. The pre-hydrothermal sample treated at 100°C has a Voc value of 117 mV and a band-gap energy of 3.340 eV, whereas the sample treated at 150°C has a Voc of 160 mV and a band-gap energy of 3.332 eV. Lastly, the aerogel sample has a Voc value of 21 mV and a band-gap-energy value of 3.329 eV.

The Voc values are related to the band-gap energies of the samples, which is due to the capability of the materials to absorb the light spectra emitted from the test projector lamp, which has a specific spectral composition. In general, higher band gaps tend to absorb shorter wavelength spectra (blue shift); therefore, our results reveal that the Voc value is in favor of a longer wavelength spectrum.

Our Voc results show that the pre-hydrothermal sample prepared at 120°C has the highest band-gap-energy value. According to the literature, the higher the temperature of the hydrothermal process, the higher the Voc value of the obtained material. However, in this case, anomalies seem to occur at higher temperatures and there is a decrease in yield for the samples treated at

150°C. This deviation could be the effect of a random variable in this research, namely, the thickness of the TiO<sub>2</sub> layer on the conductive glass.

Our results suggest that pre-hydrothermal treatment can make stiff Ti–OH networks become more flexible, leading to the formation of Ti–O–Ti arrangements after completion of the hydrolysis process. These Ti–O–Ti structures improve the crystallinity of TiO<sub>2</sub> and lead to a better performance of the material. The presence of a stiff Ti–OH network in the aerogel affects the crystallinity of the material and hinders the formation of Ti–O–Ti arrangements. Thus, Ti–O–Ti networks are better distributed in hydrothermally treated samples than in the aerogel. The highest Voc value was observed for the pre-hydrothermally treated sample obtained at 120°C, which indicates that the optimum conditions were achieved at this temperature.

#### 4. CONCLUSION

All the samples resulting from this research had a nanocrystalline structure and were successfully assembled into DSSCs to study their ability to convert light into electrical energy, as shown by their Voc values.

The properties of the TiO<sub>2</sub> aerogel reported herein exceeded those of materials presented in previous research, exhibiting a larger surface area and achieving a high enough crystallinity. Furthermore, compared to samples submitted to pre-hydrothermal treatment, the aerogel had the highest surface area (110.31 m<sup>2</sup>/g) and a crystallite size of 8.07 nm.

Regarding the crystallite size, the largest structures were obtained by pre-hydrothermal treatment at 150°C (9.73 nm), with a surface area of 82.17 m<sup>2</sup>/g. The size of the samples treated at 120°C was 7.79 nm (surface area: 85.43 m<sup>2</sup>/g) and that of the materials treated at 100°C was 7.45 nm (in this case the surface area was only 71.31 m<sup>2</sup>/g). Pre-hydrothermal treatment was performed to suppress the fast development of stiff Ti–OH structures, which lead to largely amorphous particles. This treatment transforms the Ti–OH network into a flexible Ti–O–Ti arrangement. Subsequent multi-step calcination enhances the crystallinity of the resulting TiO<sub>2</sub> particles further, thus confirming the findings of previous researchers.

Voc measurements revealed that DSSCs fabricated using the aerogel provided 21 mV. The best results were obtained for the pre-hydrothermally treated sample prepared at 120°C (320 mV), followed by the samples treated at 150° and 100°C, respectively.

#### 5. ACKNOWLEDGEMENT

The authors would like to acknowledge financial support from the Directorate of Research and Community Services - Universitas Indonesia (DRPM-UI) through Hibah Riset Madya Universitas Indonesia under contract no. DRPM/RII/175/RM-UI/2013.

#### 6. REFERENCES

- Brodsky, C.J., Ko, E.I., 1994. Effect of Drying Temperature on the Physical Properties of Titania Aerogels. *Journal of Materials Chemistry*, Volume 4(4), pp. 651–652
- Dai, S., Wu, Y., Sakai, T., Du, Z., Sakai H., Abe, M., 2010. Preparation of Highly Crystalline TiO<sub>2</sub> Nanostructures by Acid-assisted Hydrothermal Treatment of Hexagonal-structured Nanocrystalline Titania/Cetyltrimethylammonium Bromide Nanoskeleton. *Nanoscale Research Letters*, Volume 5(11), pp. 1829–1835
- Ge, L., Xu, M., Fang, H., Sun, M., 2006. Preparation of TiO<sub>2</sub> Thin Films from Autoclaved Sol Containing Needle-like Anatase Crystals. *Applied Surface Science*, Volume 253(2), pp. 720–725

- Khan, M.Z.H., Al-Mamun, M.R., Halder, P.K., Aziz, M.A., 2017. Performance Improvement of Modified Dye-sensitized Solar Cells. *Renewable and Sustainable Energy Reviews*, Volume 71, pp. 602–617
- Kim, D.S., Han, S.J., Kwak, S.Y., 2007. Synthesis and Photocatalytic Activity of Mesoporous TiO<sub>2</sub> with the Surface Area, Crystallite Size, and Pore Size. *Journal of Colloid and Interface Science*, Volume 316(1), pp. 85–91
- Langlet, M., Kim, A., Audier, M., Herrmann, J.M., 2002. Sol-Gel Preparation of Photocatalytic TiO<sub>2</sub> Films on Polymer Substrates. *Journal of Sol-Gel Science and Technology*, Volume 25(3), pp. 223–234
- Naghibi, S., Sani, M.A.F., Hosseini, H.R.M., 2014. Application of the Statistical Taguchi Method to Optimize TiO<sub>2</sub> Nanoparticles Synthesis by the Hydrothermal Assisted Sol-Gel Technique. *Ceramics International*, Volume 40(3), pp. 4193–4201
- Nursama, N.M., Muliani, L., 2012. Investigation of Photoelectrode Materials Influences in Titania-Based-Dye-Sensitized Solar Cell. *International Journal of Technology*, Volume 3(2), pp. 129–139
- O'Regan, B., Grätzel, M., 1991. A Low-cost, High-efficiency Solar-Cell based on Dye-sensitized Colloidal TiO<sub>2</sub> Films. *Nature*, Volume 353, pp. 737–740
- Priyono, B., Yuwono, A.H., Munir, B., Rahman, A., Maulana, A., Abimanyu, H., 2013. Synthesis of Highly-ordered TiO<sub>2</sub> through CO<sub>2</sub> Supercritical Extraction for Dye-sensitized Solar Cell Application. *Advanced Materials Research*, Volume 789, pp. 28–32
- Schneider, M., Baiker, A., 1997. Titania-based Aerogels. *Catalysis Today*, Volume 35(3), pp. 339–365
- Slamet, Nasution, H.W., Purnama, E., Kosela, S., Gunlazuardi, J., 2005. Photocatalytic Reduction of CO<sub>2</sub> on Copper-doped Titania Catalysts Prepared by Improved-impregnation Method. *Catalyst Communications*, Volume 6(5), pp. 313–319
- Sofyan, N., Ridhova, A., Yuwono, A.H., Udhiarto, A., 2017. Fabrication of Solar Cells with TiO<sub>2</sub> Nanoparticles Sensitized using Natural Dye Extracted from Mangosteen Pericarps. *International Journal of Technology*, Volume 8(7), pp. 1229–1238
- Sugathan, V., John, E., Sudhakar, K., 2015. Recent Improvements in Dye Sensitized Solar Cells: A Review. *Renewable and Sustainable Energy Reviews*, Volume 52, pp. 54–64
- Wang, C.-C., Ying, J.Y., 1999. Sol-Gel Synthesis and Hydrothermal Processing of Anatase and Rutile Titania Nanocrystals. *Chemical Materials*, Volume 11(11), pp. 3113–3120
- Yuwono, A.H., Munir, B., Ferdiansyah, A., Rahman, A., Handini, W., 2010. Dye Sensitized Solar Cell with Conventionally Annealed and Post Hydrothermally Treated Nanocrystalline Semiconductor Oxide TiO<sub>2</sub> Derived from Sol-Gel Process. *Makara Journal of Technology*, Volume 14(2), pp. 53–60
- Yuwono, A.H., Xue, J., Wang, J., Elim, H.I., Ji, W., 2006. Titania-PMMA Nanohybrids of Enhanced Nanocrystallinity. *Journal of Electroceramics*, Volume 16(4), pp. 431–439